

Hydration evolution of C₃S–EVA composites analyzed by soft X-ray microscopy

D.A. Silva*, P.J.M. Monteiro

Department of Civil and Environmental Engineering, University of California at Berkeley, USA

Received 26 February 2004; accepted 27 May 2004

Abstract

The effect of poly(ethylene-co-vinyl acetate) or EVA on the hydration of a pure C₃S was investigated by transmission soft X-ray microscopy in highly diluted systems. EVA particles are readily recognizable by their spherical shape and semitransparency to soft X-rays. Polymeric particles adsorb on the surface of hydrating C₃S grains, and act as nucleation agents in the development of the composite microstructure. The formation of a polymeric film was observed after a few hours of hydration. Fourier-transform infrared spectroscopy supported the conclusions that a highly soluble phase is formed as a result of EVA-hydrating C₃S chemical interactions.

© 2004 Elsevier Ltd. All rights reserved.

Keywords: Cement paste; EVA copolymer; Soft X-ray microscopy; C–S–H; Microstructure

1. Introduction

Poly(ethylene-co-vinyl acetate), or simply EVA copolymer, is added to mortars and concretes during mixing to improve properties, such as elastic modulus, toughness, impermeability and bond strength to various substrates [1] as well as water retention capacity and plasticity in the fresh state [2]. EVA redispersible polymer powder can be added to anhydrous cement and aggregates before mixing with water, or it can be added during the mixing as an aqueous dispersion. Due to improved adhesion, it is also used for the production of dry-set mortars for ceramic tile installation, especially for coating of facades, which are frequently exposed to severe environmental conditions, including temperature, humidity, and stress cycles. Thus, it is relevant to investigate the role of EVA in cement-based materials in order to establish their structure–properties relationships.

The effect of EVA on the hydration of cement has been investigated by various researchers using known experimental techniques in materials science. Afridi et al. [3] used scanning electron microscopy and X-ray diffraction to study the effect of EVA on various hydrated phases, such as

calcium hydroxide and aluminate phases. Silva et al. [4] showed evidence of chemical interaction of the acid groups released by the partial alkaline hydrolysis of EVA with Ca²⁺ ions in the pore water of the cement pastes through infrared spectroscopy and thermal analysis. On the other hand, Sakai and Sugita [5], using cryo-SEM to explain the composite mechanism of EVA-modified pastes, observed that the spherical polymeric particles were not altered by the cement hydration, but filled the interface between the cement particles. However, this technique did not allow the authors to conclude if any kind of chemical interaction occurred between the polymeric and cementitious particles, leading them to claim for further investigation on the subject.

Although the abovementioned research improved the knowledge of the basic mechanics of cement–polymer composites, the techniques used so far have not clarified the effects of EVA on the cement hydration mechanism and products beyond the first few minutes of hydration. The high vacuum applied on the sample for the SEM analysis can affect the morphology of the hydrated phases, specially the C–S–H, which is extremely sensitive to moisture [6]. Although Sakai and Sugita's [5] research through cryo-SEM focused on the comparison of the polymeric particles dispersion in EVA-modified cements immediately after mixing and at the age of 3 days, their research did not focus the microscopic analysis on the nucleation and growth of hydrated phases.

* Corresponding author. Department of Civil Engineering, Federal University of Santa Catarina, Caixa Postal 476, CEP 88040-900, Florianópolis SC, Brazil. Tel.: +55-48-331-5176; fax: +55-48-331-5191.

E-mail address: denise@ecv.ufsc.br (D.A. Silva).

The transmission soft X-ray microscopy described in this paper has proven to be an important tool to fill this gap in the knowledge regarding cement–EVA composites. Because the sample was subjected to atmospheric pressure, there was no drying due to low pressures. Wet samples were analysed, allowing the observation of cement hydration in real time. Furthermore, the internal microstructure of hydrated phases is evident [7].

Because portland cement is a quite complex material composed by many reactive phases, any statement about the nature of chemical reactions of its phases and other reactive compounds must be made carefully. To better understand the influence of EVA on portland cement hydration, its main compound— C_3S —was synthesized, ground and mixed with the copolymer. The development of the hydrated phases beyond the very few minutes of hydration was followed by soft X-ray microscopy of highly diluted dispersions. This study concentrated primarily on the morphology of the hydrated phases, the rate of particle dissolution, and growing and the overall particle distribution. The microscopic observation was accomplished using infrared spectra obtained from identical samples.

2. Materials and methods

A pure C_3S was synthesized, ground, and sieved to study the microstructural development of cement–polymer composites. Particles with dimensions smaller than $37\ \mu\text{m}$ were selected for the tests.

A commercial EVA redispersible polymer powder was used, whose characteristics are presented in Table 1. The inorganic part (ash content) of the commercial EVA contains the minerals magnesite (37% mass of the inorganic compounds), dolomite (13%), calcite (14%), talc (16%) and kaolinite (20%), identified and semiquantified using XRD analysis. EVA redispersible polymer powder was sieved to reduce the amount of inorganic phases in the mixtures, and particles with diameters between 75 and $37\ \mu\text{m}$ were selected for the analysis.

The techniques used to investigate the microstructural development of C_3S –EVA composites were soft X-ray transmission microscopy and infrared spectrometry on highly diluted solutions/dispersions of EVA and/or C_3S .

The soft X-ray transmission microscope, built and operated by the Center of X-rays Optics (Advanced Light

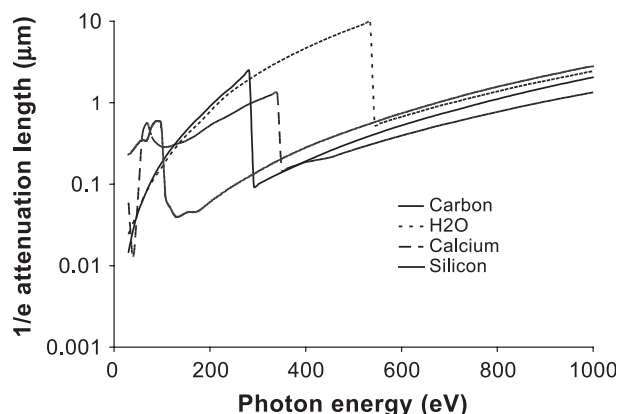


Fig. 1. Attenuation length versus photon energy for water, carbon, calcium, and silicon. The photon energy used for the whole analysis was 517 eV.

Source, Lawrence Berkeley National Laboratory, Berkeley, CA), was first used to study cement-based materials by Kurtis [8]. The technique allows the observation in situ of wet samples at normal pressures with high resolutions (up to $43\ \text{nm}$). The incident X-rays pass through the sample where they are partially absorbed with a spatial variation dependent on the atoms present (atomic number Z), their distribution and the wavelength of the incident rays (λ) [9]. Fig. 1 shows the attenuation length (or absorption) versus photon energy for water, carbon, calcium and silicon. The microscopy was carried out using photon energy of 517 eV, corresponding to a wavelength of $2.4\ \text{nm}$. Because the photon energy is above the K absorption edge for carbon (284.2 eV), the polymer particles are not transparent to soft X-rays. They can be readily recognized by their shape (spherical) and semitransparency. Calcium, carbon and silicon absorb almost the same radiation, but the contrast of the phases containing such elements to the water depends on the composition of the phase (content of each element) and the thickness of the particles. For the samples analyzed here, polymeric particles are semitransparent while Ca- and Si-bearing phases are dark.

Further details about the optics features of the synchrotron radiation and the X-ray microscope are given elsewhere [9,10].

Due to the thickness restriction of the sample (up to $10\ \mu\text{m}$), the solid particles must be dispersed in a liquid media and then centrifuged for the analysis. Therefore, a saturated solution composed of calcium hydroxide (CH) and gypsum (pH = 12.3) was prepared with fresh, boiled deionized water. After homogenization and double filtering with filter papers, the solution was placed inside polyethylene flasks, and tightly closed. To avoid carbonation, the entire preparation of the solution was made inside a glove bag filled with N_2 gas. Juenger et al. [11] used this solution instead of deionized water to decrease the kinetics of hydration of portland cement, allowing more time to prepare the mixtures and assemble the samples without prejudice to the analysis.

Table 1

Characteristics of EVA redispersible polymer powder

Ash content (30 min at $1000\ ^\circ\text{C}$)	13.0%
Apparent density (DIN 53189)	472 g/l
Particle size	$75\ \mu\text{m} > \phi > 37\ \mu\text{m}$
Protective colloid	Poly(vinyl alcohol)
Minimum film forming temperature	Approximately $4\ ^\circ\text{C}$
pH of EVA dispersion in deionized water, 25% mass	9.1

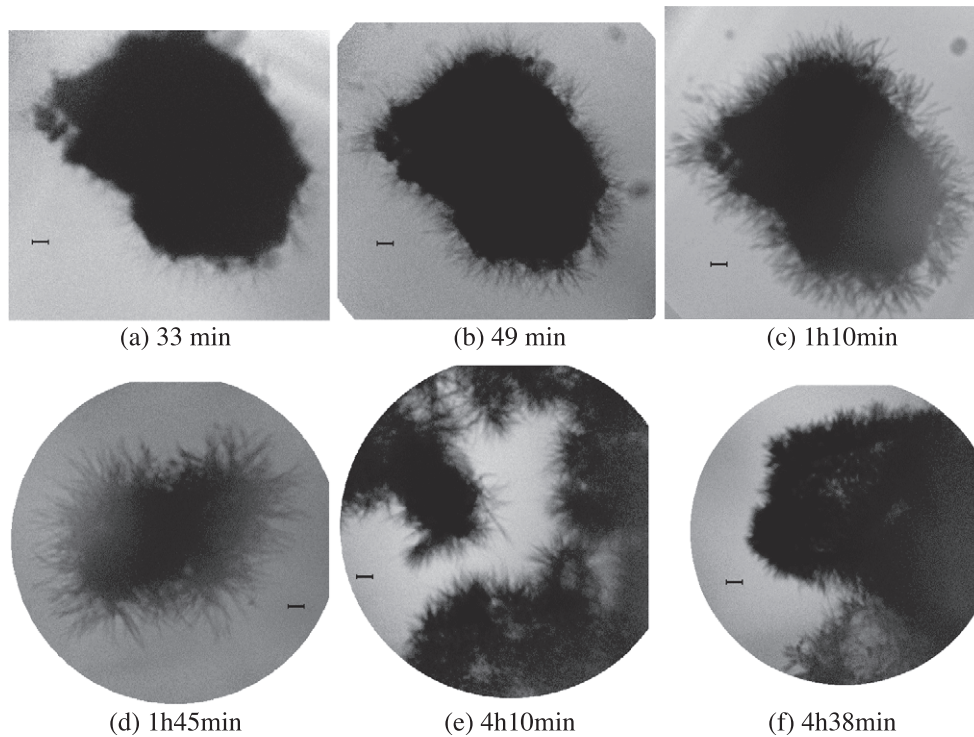


Fig. 2. X-ray images of hydrating C_3S particles in CH-gypsum saturated solutions from 33 min to more than 4 h of hydration. Panels (a) to (c) are images of the same particle. Panels (e) and (f) are different particles of the same sample. Panel (d) is from another sample (scale bar is 700 nm).

EVA and/or C_3S were added to the saturated solutions. The EVA/water ratios were in the range $0.02\text{--}0.04\text{ g/cm}^3$, and the water/ C_3S ratios were 5, 14, and $50\text{ cm}^3/\text{g}$. The mixtures were agitated for not more than 1 min and immediately centrifuged for 10 s, following the experimental procedure adopted by Juenger et al. [11]. A small droplet taken from the supernatant solution was assembled in the sample holder between two silicon nitride windows for the analysis. The analysis was performed from the very beginning of reaction (few minutes) until some hours after the mixture.

To detect the evidence of eventual chemical interactions of the hydrating C_3S and EVA, a C_3S –EVA solution (water/ C_3S =5, EVA/water=0.02) was prepared and analyzed by Fourier-transform infrared spectroscopy. A small droplet of the sample was squeezed between two sodium chloride pellets. Spectra were obtained at 5, 25, 45, 60, and 120 min after mixing. An ATI Mattson-Infinity Series FTIR Fourier-transform infrared spectrometer was used. The spectra were obtained in the range $4000\text{--}400\text{ cm}^{-1}$ but traced only in the range $2000\text{--}1200\text{ cm}^{-1}$ (wave number), and the band intensities were expressed in transmittance

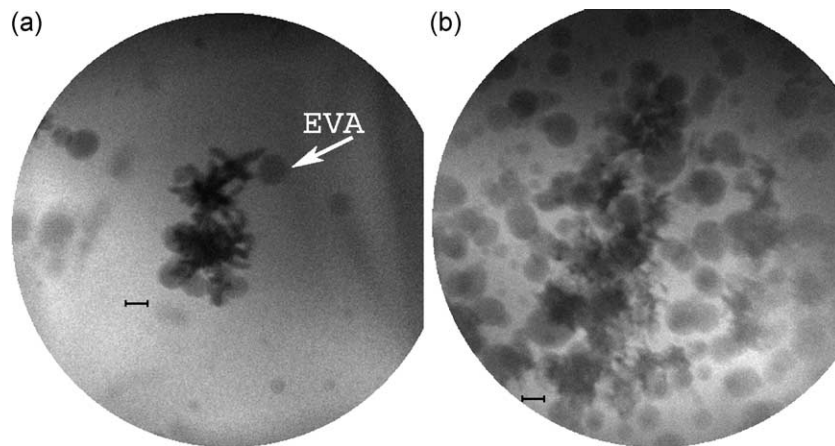


Fig. 3. X-ray images of hydrating C_3S particles and EVA spheres in CH-gypsum saturated solution. (a) Water/ C_3S ratio is 50 and EVA/water ratio is 0.028, 3 h after mixing; and (b) water/ C_3S ratio is 14 and EVA/water ratio is 0.043, 4 h after mixing (scale bar is 700 nm).

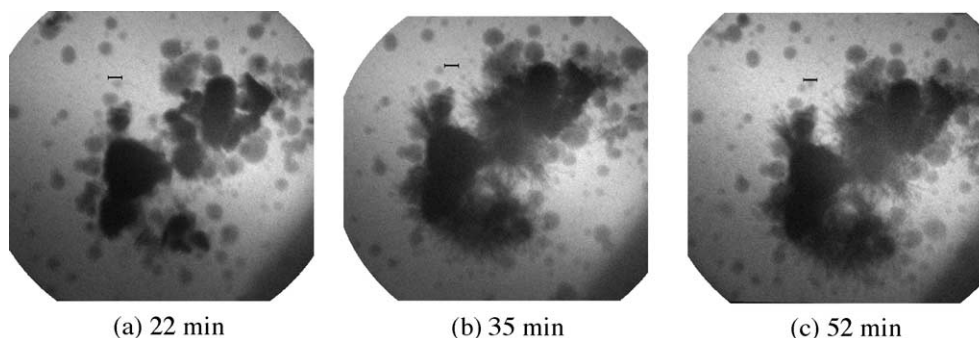


Fig. 4. X-ray images of hydrating C_3S particles and EVA spheres. Water/ C_3S ratio is 5 and EVA/water ratio is 0.02, hydration time indicated (scale bar is 700 nm).

(%). The infrared analysis permitted identification of the main molecular groups present in the solutions, and the discussion of these results is presented below.

3. Results

Fig. 2 shows some X-ray images of hydrating C_3S particles in CH-gypsum saturated solution from 33 min to almost 5 h of hydration. As can be seen, numerous thin needles of hydrated products grow from the surface of hydrating C_3S particles forming a hydrated layer; Juenger et al. [11] observed similar phenomena. This process starts within few minutes after mixing. The configuration shown in Fig. 2 does not change very much after some tens of minutes, which is not surprising as further nucleation and growing of hydrated particles are rate controlled by the ability of the solvated ions to cross the hydrated layer. Furthermore, there is a tendency of Hadley grains to be formed. It is possible to distinguish a flat Hadley grain in Fig. 2f, with the characteristic outer and inner C-S-H. No hydrated crystals were detected away from the original C_3S particle, which is most likely due to the high dilution of the system and to the absence of nucleation agents.

Figs. 3 and 4 show the C_3S particles hydrating in the presence of EVA in solutions with different solid contents. The polymeric particles are recognizable by their spherical

shape and by the semi transparency compared to the inorganic phases, whose atoms have higher Z (atomic number) than carbon and provide to the particles more contrast to the aqueous phase. EVA particles are able to disperse evenly in both deionized water and CH-gypsum saturated solution. The diameter of EVA particles is 1 μm or less, but it is important to consider that larger particles could have been dislocated from the supernatant dispersion during centrifugation. It appears that the high pH of the saturated solution (12.3) did not affect the redispersion of EVA particles when analyzed by the transmission soft X-ray microscope.

When EVA is added to C_3S dispersions, it tends to concentrate around cementitious particles at the very beginning of hydration regardless the solids content of the dispersion (see Figs. 3–5). Hydrated needles growing from C_3S surface can be seen in Fig. 4, forming the sheaf-of-wheat morphology previously recognized by Juenger et al. [11]. The formation of spherulites is shown in Fig. 5; however, most of the hydrated needles seem to be thicker than the ones that grew in the system without EVA. The needles are either growing on or are being surrounded by EVA particles. Figs. 3 and 5c demonstrate that hydrated crystals also precipitate far away from the original C_3S particles when EVA is added to the system, following the through solution mechanism of hydration. Thus, it can be concluded that EVA particles are nucleation sites for C-S-H

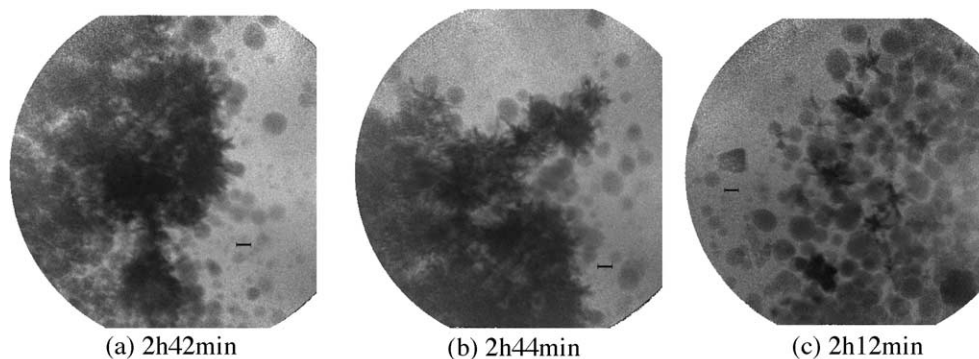


Fig. 5. X-ray images of hydrating C_3S particles and EVA spheres in CH-gypsum saturated solution. Water/ C_3S ratio is 5 and EVA/water ratio is 0.043 (scale bar is 700 nm).

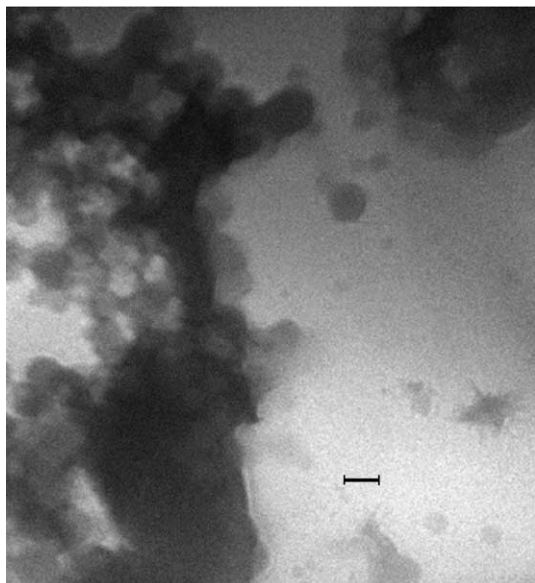


Fig. 6. X-ray image of EVA film formed in CH-gypsum saturated solution. Sample was allowed to dry overnight (scale bar is 700 nm).

crystals due to their small size (around 1 μm diameter or less) and surface activity (high polarity). The higher the number of nuclei formed, the smaller the final crystal size.

It was also observed that EVA is able to form film when dispersed in deionized water and in CH-gypsum saturated solution regardless of the presence of C_3S . The film is formed in locations where the concentration of polymeric particles is high enough to produce a continuous media. Fig. 6 shows the X-ray image of an EVA film formed in a CH-gypsum saturated solution allowed to dry overnight. The sample shown in Fig. 7, however, contains C_3S , and is only 4 h old. The small hydrated particles precipitated through solution on EVA particles are incorporated into the film. Their growth is probably imparted as a result of the film covering.

Fig. 8 shows the infrared spectra of a C_3S –EVA–solution system hydrated for up to 2 h. The band at around 1540 cm^{-1} is caused by the stretching vibration of the C–O

bond of the carboxylate anion (COO^-), whose presence is due to the alkaline hydrolysis of EVA (see Silva et al. [4]). As a consequence of an eventual total hydrolysis, the band caused by the carbonyl bond (CO) at around 1740 cm^{-1} should not appear; however, as can be seen in Fig. 8, the band is still in the spectra, meaning that the hydrolysis of the copolymer was not complete after 2 h of reaction.

The anion formed by the alkaline hydrolysis of EVA is CH_3COO^- . Because of the attachment of OH groups to the main chain of the copolymer, poly(vinyl alcohol), PVA is formed as a product of the hydrolysis as well, and the copolymer chain is converted into a terpolymer formed by the ethylene, vinyl acetate, and vinyl alcohol monomers. Furthermore, PVA is present in EVA as a protective colloidal as pointed out in Table 1.

4. Discussion

The alkaline hydrolysis of vinyl acetate is done through saponification, where the carbonyl carbon atom is the initial point of attack by the alkaline environment. The reaction causes the release of CH_3COO^- ions in solution and the formation of poly(vinyl alcohol) in the polymer chain, as discussed previously. Davies and Reynolds [12] have performed tests on the alkaline hydrolysis of poly(vinyl acetate), and concluded that the polymer rapidly hydrolyzes to 91% after 24 h exposed to a 1 N KOH solution (pH = 14). Ethylene copolymerization decreases the alkaline hydrolysis of vinyl acetate group, which is probably due to several factors, i.e., modification of local or overall water solubility or water insolubility of the macromolecule, steric protection by both side chains and the polymer backbone, and interruption of the sequence of hydrolysable units in the copolymer [12]. The higher the ethylene content, the lower the hydrolysis, but the phenomenon still occurs with ethylene content as high as 24% (on weight basis).

The hydrolysis of EVA causes changes in some properties of the copolymer, such as the melting point and the degree of crystallinity [13]. Because the $-\text{OH}$ group repla-

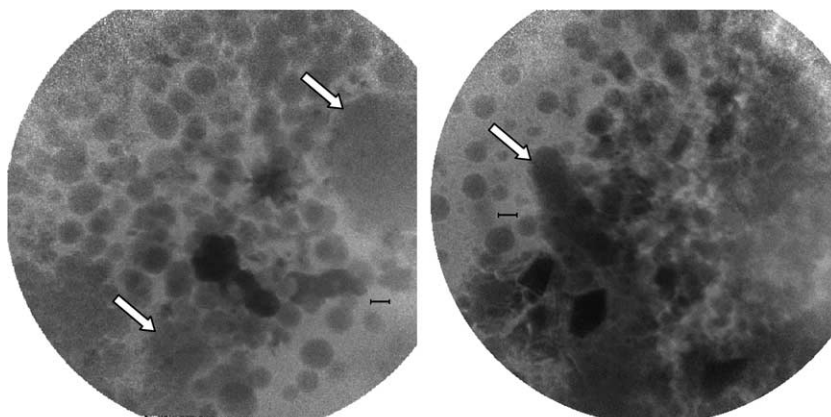


Fig. 7. X-ray images of EVA film formation after 4 h of C_3S hydration (scale bar is 700 nm).

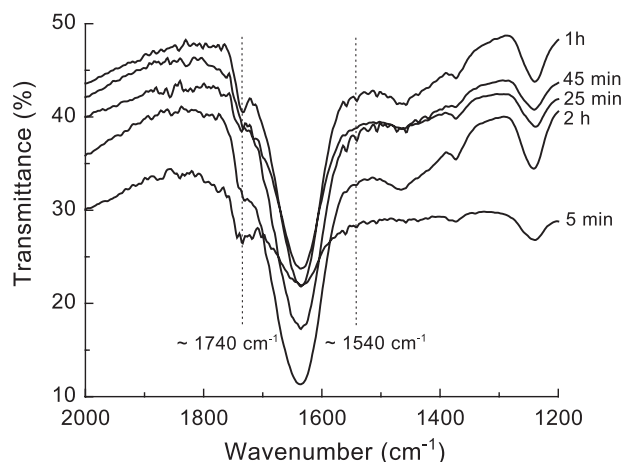


Fig. 8. FTIR spectra of C_3S -EVA dispersions from 5 min to 2 h after the mixture.

ces the $-COOCH_3$ ester group, the resulting polarity is increased [14]. As already stated, the infrared spectra shown in Fig. 8 is evidence of the partial alkaline hydrolysis of EVA particles in C_3S -EVA dispersion, meaning that the polarity of the EVA particles was increased due to the higher availability of the $-OH$ group that turns the polymeric particles hydrophilic.

Because of the residual positive charge of the surface of C_3S particles in solution [15] and to the formation of an electrical double layer on the polymer particles in an ionizing medium [1], the polymeric particles are adsorbed onto them as seen in Figs. 3–5. A comparison of Figs. 2 and 4 demonstrates that the adsorbed polymeric particles reduce the rate of C_3S dissolution. On the other hand, as seen in Figs. 3 and 5c, EVA particles probably act as nucleation sites for C_3S hydrated products anticipating the microstructural development. The overall effect of EVA on the kinetics of hydration was discussed by Silva [16] through conduction calorimetric tests, where it was shown that EVA increases the heat evolution during the first 2 h of cement hydration compared to an unmodified cement paste, leading to the conclusion that the nucleation effect of EVA particle is more important than their adsorption during the first hours of hydration. However, the adsorption of EVA onto both hydrating particles and hydration products and the film formation inhibit the growth of C-S-H and CH phases, decreasing the heat evolution [16].

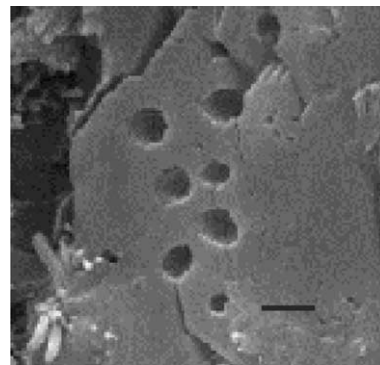


Fig. 10. Geometric calcium-bearing particle containing holes in EVA-modified cement paste, observed by scanning electron microscopy [16]. Scale bar is 1 μm .

The alkaline hydrolysis of EVA in portland cement systems releases anions (CH_3COO^-) that can combine with metallic cations (Ca^{2+} , K^+ , Na^+) from the dissolved clinker phases to form organometallic compounds. Silva et al. [4] have shown the decreased amount of $Ca(OH)_2$ in EVA-modified portland cement pastes, and have attributed the phenomenon to the consumption of Ca^{2+} ions for the formation of calcium acetate. In the samples analyzed in this research, some geometric particles having holes like a Swiss cheese were observed to form and to dissolve very fast. Fig. 9 shows a sequence of images taken during the analysis of a solution with a water/ C_3S ratio of 5 and an EVA/water ratio of 0.043, around 2 h after mixing. The particle shown in Fig. 9 is similar to the ones observed by Silva [16] in EVA-modified cement pastes (Fig. 10). Because it is well known that calcium acetate has high water solubility (34.7 g/100 g H_2O at 20 °C), the particles shown in Fig. 9 might be calcium acetate particles or other composite phase highly soluble in water.

Some of the Ca^{2+} ions can also be bound to the hydroxyl groups introduced in the polymeric chain by the alkaline hydrolysis. Besides chemical bonding (chelating) to the polymer structure, Ca^{2+} ions in solution can be physically entrapped to the polymer by the bridging effect of the water molecules through hydrogen bonding to the cations chemically bound to the hydroxyls and acetate groups. If the water is taken off from the system, the polymeric chains get closer, reducing even more the ionic mobility [17]. Many cations can be kept indefinitely in the entangled polymer

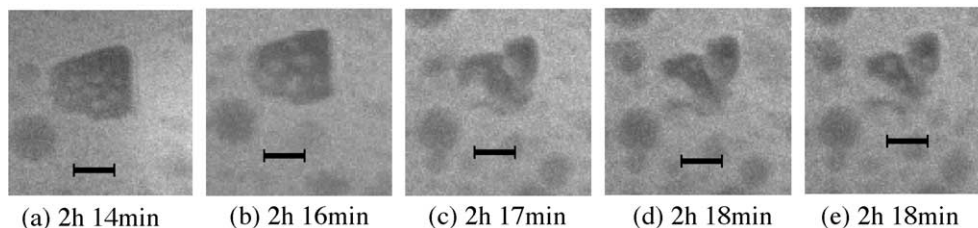


Fig. 9. X-ray images of a geometric particle containing holes and dissolving in EVA- C_3S dispersion. The age of the dispersion is indicated. Scale bar is 700 nm.

network, hindering the precipitation of calcium-bearing hydrated phases.

The consumption or entrapment of Ca^{2+} ions by the polymeric phase is likely to affect the formation of calcium silicate hydrates. The altered morphology of the needles shown in Figs. 3–5 compared to the ones shown in Fig. 2 may be the evidence of a distinct composition of the hydrated phases when EVA is present in the system. It is possible that some polymeric group have been incorporated between C-S-H layers [18], increasing the needles' thickness. Some XRD tests are currently being performed in an attempt to detect such incorporation.

5. Conclusions

Soft X-ray transmission microscopy is a valuable technique to observe the hydration of cementitious particles under the influence of EVA latex. The use of Fourier-transform infrared spectroscopy contributed to significant new understanding of important aspects of the interaction of hydrating C_3S and EVA.

It was shown that EVA copolymer hydrolyzes in the alkaline environment of hydrating C_3S , releasing CH_3COO^- in solution. The resulting surface activity of polymeric particles leads them to adsorb onto hydrating C_3S particles that have hindered their dissolution, as well as the hydrated crystals growing. On the other hand, EVA particles are nucleation sites for hydrated phases, hastening the precipitation process.

The anions released by the alkaline hydrolysis of EVA can form organometallic compounds with Ca^{2+} ions in solution, changing the Ca/Si ratio of C-S-H and reducing the amount of calcium hydroxide. Furthermore, the anions CH_3COO^- can be incorporated between the layers of C-S-H, thereby increasing the space between them. The presence of PVA may lead to the adsorption or incorporation of $-\text{OH}$ group between the layers [18]; the thicker hydrated needles observed through soft X-ray microscopy may be due to such interaction. X-ray diffraction analysis is currently being performed to investigate the phenomenon.

Acknowledgements

The authors acknowledge the financial support of CAPES (Fundação Coordenação de Aperfeiçoamento de Pessoal de Nível Superior-Ministério da Educação-Brasil) and are grateful to Dr. Angelic Pearson of the Center for X-ray Optics and the Lawrence Berkeley National Laboratory for her assistance in acquiring the images. Research at XM-1 is supported by the United States Department of Energy, Office of Basic Energy Sciences under contract DE-AC 03-

76SF00098. The authors are also grateful to Richard Brutchey and Prof. Don Tilley from the Department of Chemistry, University of California at Berkeley. The research was supported by the National Science Foundation and the Federal Highway Administration (grant CMS-981275).

References

- [1] S. Chandra, Y. Ohama, *Polymers in Concrete*, CRC Press, Boca Raton, FL, 1994.
- [2] M.U.K. Afridi, Y. Ohama, M.Z. Iqbal, K. Demura, Water retention and adhesion of powdered and aqueous polymer-modified mortars, *Cem. Concr. Compos.* 17 (1995) 113–118.
- [3] M.U.K. Afridi, Y. Ohama, M.Z. Iqbal, K. Demura, Behaviour of $\text{Ca}(\text{OH})_2$ in polymer modified mortars, *Int. J. Cem. Comp. Light-weight Concr.* 11 (1989) 235–244.
- [4] D.A. Silva, H.R. Roman, P.J.P. Gleize, Evidences of chemical interaction between EVA and hydrating Portland cement, *Cem. Concr. Res.* 32 (2002) 1383–1390.
- [5] E. Sakai, J. Sugita, Composite mechanism of polymer modified cement, *Cem. Concr. Res.* 25 (1995) 127–135.
- [6] M.C.G. Juenger, Quantifying microstructural variations in cement pastes: Implications on drying shrinkage, Northwestern University, Dissertation, 1999.
- [7] E.M. Gartner, K.E. Kurtis, P.J.M. Monteiro, Proposed mechanism of C-S-H growth tested by soft X-ray microscopy, *Cem. Concr. Res.* 30 (2000) 817–822.
- [8] K.E. Kurtis, Transmission soft X-ray microscopy of the alkali-silica reaction, PhD dissertation, Department of Civil and Environmental Engineering, University of California, Berkeley, CA, 1998.
- [9] D. Atwood, *Soft X-Rays and Extreme Ultraviolet Radiation: Principles and Applications*, Cambridge Univ. Press, University of California-Berkeley/LBNL, New York, 1999.
- [10] K.E. Kurtis, W. Meyer-Ilse, P.J.M. Monteiro, Soft X-ray spectromicroscopy for in situ study of corrosion, *Corros. Sci.* 43 (2000) 1327–1336.
- [11] M.C.G. Juenger, V.H.R. Lamour, P.J.M. Monteiro, E.M. Gartner, G.P. Denbeaux, Direct observation of cement hydration by soft X-ray transmission microscopy, *J. Mater. Sci. Lett.* 22 (2003) 1335–1337.
- [12] R.F.B. Davies, G.E.J. Reynolds, Alkaline hydrolysis of aqueous polymer dispersions, particularly vinyl acetate copolymers, *J. Appl. Polym. Sci.* 12 (1968) 47–58.
- [13] E. Corradini, A.F. Rubira, E.C. Muniz, Miscibility of PVC/EVA hydrolyzed blends by viscosimetric, microscopic and thermal analysis, *Eur. Polym. J.* 33 (1997) 1651–1658.
- [14] X.M. Xie, T.J. Xiao, Z.M. Zhang, A. Tanioka, Effect of interfacial tension on the formation of the gradient morphology in polymer blends, *J. Colloid Interface Sci.* 206 (1998) 189–194.
- [15] R.M. Edmeades, P.C. Hewlett, Cement admixtures, in: P.C. Hewlett (Ed.), *Lea's Chemistry of Cement and Concrete*, Arnold, London, 1998, pp. 837–902.
- [16] D.A. Silva, Effects of EVA and HEC polymers on the microstructure of Portland cement pastes, UFSC/PGMAT dissertation, Florianopolis-Brazil, 2001 (in Portuguese).
- [17] M.A. Gülgün, M.H. Nguyen, W.M. Kriven, Polymerized organic-inorganic synthesis of mixed oxides, *J. Am. Ceram. Soc.* 82 (3) (1999) 556–560.
- [18] H. Matsuyama, J.F. Young, Synthesis of calcium silicate hydrate/polymer complexes: Part I. Anionic and nonionic polymers, *J. Mater. Res.* 14 (8) (1999) 3379–3388.